

CONDENSATION HEAT TRANSFER COEFFICIENTS OF ENHANCED TUBES

Ewim D.R.E. and Meyer J.P.*

Department of Mechanical and Aeronautical Engineering,
 University of Pretoria,
 Pretoria, 0002,
 South Africa

E-mail: josua.meyer@up.ac.za

ABSTRACT

In solar power generating plants, dry cooling towers are used when there is scarcity of water. Normally, condensation of the steam occurs in dry cooling towers in tubes at inclined angles. Almost all the previous work on condensation was in horizontal and vertical tubes until recently when work was done on condensation in inclined tubes but limited to smooth tubes and one type of enhanced tube. The purpose of this paper is to continue on previous work and present heat transfer coefficients and pressure drops during the condensation of R134a in an enhanced tube of inner diameter of 8.67mm with 60 fins with height of 0.22mm spiraled at an angle of 37°. The experiments were conducted at condensing temperatures of 30°C and 40°C at mass fluxes between 300 kg/m²s and 400 kg/m²s and various vapour qualities. It was found that the heat transfer coefficients and pressure drops increased with mean quality. Overall, the heat transfer enhancement factors were between 2.1 and 2.9 and the pressure drop penalty factors were between 1.2 and 1.8 with the enhancement more pronounced at lower mass fluxes. Finally, the heat transfer and pressure drops increased with decrease in condensing temperature.

INTRODUCTION

Condensation of steam occurs in tubes at different angles of inclination in dry cooling towers which find application in solar powered generating plants. Previous studies by Lips and Meyer [1], Meyer *et al.* [2], Adelaja *et al.* [3] and Akhavan-Behadabi *et al.* [4] have either been on smooth tubes or enhanced tubes with spiraled fins at low helix angles.. In these studies, the effect of tube inclination was found to be more significant at low vapour qualities and low mass fluxes. Furthermore, the tube orientation influenced the flow pattern and altered the position of the liquid phase. Many other studies [4-10] have been carried out on the effects of enhanced tube surfaces on the heat transfer, pressure drops and flow patterns. Comparisons have been made against smooth tubes and to summarize, enhanced tubes give about 80-180% increase in heat transfer with a corresponding increase in pressure drop in the region of 20-80% [6-11]. However, there is a need for more empirical studies on convective condensation in other enhanced tubes with higher helix angles and covering the whole range of vapour qualities at different saturation temperatures. In this paper, heat transfer enhancement and pressure drop penalty

factors are presented for micro fins at 37° helix angle. Few experimental studies have been conducted on convective condensation in enhanced tubes at different saturation temperatures and numerical work is very complex because of the prevailing two-phase phenomenon. Thus, a lacuna exists in the literature which hinders the design of efficient condensers. This paper aims to bridge that gap and will be very useful to research and design engineers. It is imperative to note that even though the working fluid used in this study is R134a as against steam due to the design features of our set-up, the qualitative results are relevant to that of steam. However, it will be worthwhile to design a condensation experimental set-up running on steam in the near future.

NOMENCLATURE

<i>A</i>	area (m ²)
<i>C_p</i>	specific heat (J/kg.K)
<i>d</i>	diameter (m)
<i>EB</i>	energy balance
<i>g</i>	gravitational acceleration (m ² /s)
<i>G</i>	mass flux (kg/m ² s)
<i>h</i>	enthalpy (J/kg)
<i>k</i>	thermal conductivity (W/mK)
<i>L</i>	length of test section (m)
<i>m</i>	mass flow rate (kg/m ² s)
<i>ΔP</i>	pressure drop (kPa)
<i>Q</i>	heat transfer rate (W)
<i>R</i>	thermal resistance (K/W)
<i>T</i>	temperature (°C)
<i>x</i>	vapour quality
<i>z</i>	axial direction

Greek symbols

<i>α</i>	heat transfer coefficient (W/m ² K)
----------	--

Subscripts

<i>Cu</i>	copper
<i>H₂O</i>	water
<i>i</i>	inner
<i>in</i>	inlet
<i>j</i>	measurement location
<i>l</i>	liquid
<i>mf</i>	microfin
<i>o</i>	outer
<i>out</i>	outlet
<i>pre</i>	pre-condenser
<i>ref</i>	refrigerant
<i>s</i>	smooth
<i>sat</i>	saturation
<i>test</i>	test-condenser

v vapour
w water

EXPERIMENTAL TEST-RIG AND CONDITIONS

The test bench used for this investigation is stationed at the Thermo Flow Laboratory of the Department of Mechanical and Aeronautical Engineering, University of Pretoria and a number of researchers [1-5] have published works emanating from the test rig. However for this present study, the test section was replaced. See (Table 1). The experimental test rig was made of two distinct cycles namely the vapour compression cycle and the water cycle as shown in (Fig. 1). The vapour compression cycle was made up of the test line and the bypass line which are high pressure lines and a low pressure line through which the R134a was pumped using a hermetic scroll compressor with a nominal capacity of 10 kW. Each of the lines had an electronic expansion valve (EEV) which controlled the rate of flow of the refrigerant. The test line had three condensers: the pre-condenser, the test condenser and the post condenser each having distinct functions. The pre condenser was used to control the inlet vapour quality (x) into the test condenser where the actual measurements and experiments were carried out and the post condenser was used to ensure that complete condensation and sub cooling (between 12.74 and 34.74°C). The bypass line had a bypass condenser that controlled the pressure, temperature and mass flow rate of the refrigerant flowing into and through the test line. The refrigerant from the high pressure lines were throttled in the EEVs into the low pressure line consisting of the evaporator, suction accumulator and scroll compressor.

In the water cycle, cold and hot water was supplied by a 50 kW heating and 70 kW cooling dual-function heat pump and was thermostatically regulated such that the cold water was set at between 15-20°C while the hot water was set at about 25°C. Both hot and cold water were stored in two 500 litre insulated tanks. The tanks were connected to a chiller and hot water heat pumps that maintained the water at constant temperatures.

The test section was a copper microfin tube in tube counter flow heat exchanger wherein the refrigerant flowed in the inner tube and water flowed in the annulus. (See Fig. 2). The inner tube was 1.48m in length with an outer diameter of 9.54 mm while the outer tube through which the cooling water flowed had an outer diameter of 15.9 mm. To ensure that the flow through the test condenser was fully developed, a straight calming section, 50 cm long was positioned at the entrance to the test section (after the sight glasses) and another calming section, 40 cm long was positioned at the exit of the test condenser to minimize the disturbance at the exit sight glass. The purpose of the sight glasses was to enable flow visualization and to serve as insulators against axial heat conduction. A high speed camera (200 frames per second) whose function was capturing the flow patterns was installed at the exit sight glass. The tube used in making the sight glasses was selected to have the same diameter as the microfin tube and was connected to the copper tube via a brass housing and sealed with a polytetrafluoroethylene (PTFE) thread tape to

avoid any disturbance of flow. A uniform backlight was installed against the sight glass to ensure uniformity in the distribution of the light emitting diode (LED) and this enabled good colour fidelity. Three sets of pressure taps were mounted between the sight glass and the test section on either side. Two of the taps were connected to different sensor pressure transducers to measure the absolute pressures at the inlet and outlet of the test condenser. The third set was connected to a differential pressure transducer. Flexible hoses made of nitrile and reinforced with high tensile steel wire braids and covered with synthetic rubber were used to connect the test section so that it could achieve the needed inclination angles. These hoses were selected to withstand a pressure of up to 36 MPa and a temperature of between -35°C and 105°C and to avoid energy losses, were further insulated with polyethylene pipes.

Figure 1 shows the schematic of the experimental set-up.

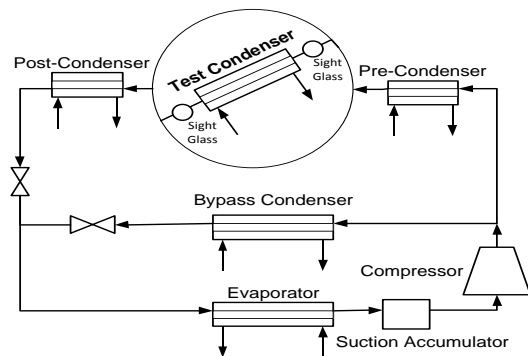


Figure 1: Schematic diagram of experimental set-up

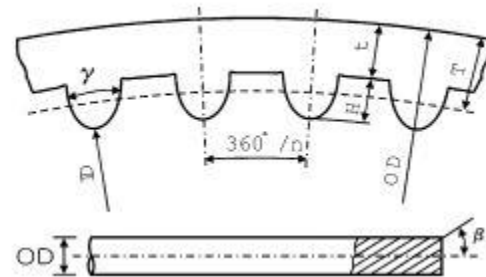


Figure 2: Geometry of a microfin tube

For the inner tube through which the refrigerant flowed, 28 grooves were made at seven positions marked (A-G) equidistant to one another along the tube. The first position was at a distance of 7 cm from the origin of the tube with a subsequent spacing of 22.5 cm after each position. Each position had four grooves marked (1-4) at equal distances around the circumference of each position where the T-type thermocouples (copper-constantan) used to measure the tube wall temperature were attached to by soldering. The

refrigerant temperature was taken at four stations: inlet and outlet of the test section, inlet of the pre-condenser and outlet of the post condenser. The consistency of these measurements was verified between the saturation temperature obtained with the absolute pressure transducer and the saturation temperature measured by the thermocouples. In consonance with the refrigerant, the cooling water inlet and outlet temperatures were measured at two stations. All the thermocouples used were calibrated against a high precision platinum resistance temperature (Pt100) detector in a thermal bath to an accuracy of $\pm 0.1^\circ\text{C}$. The refrigerant and water mass flow rates through the three condensers were measured with a coriolis mass flow meter. The refrigerant pressure at the inlet to the test condenser was measured with a strain gauge pressure transducer to an accuracy of ± 2 kPa for mass fluxes between (50-200 kgms⁻²) and 12 kPa for mass fluxes above 300 kgms⁻². To determine its accuracy, the measured pressure value was cross-checked with the corresponding saturation temperature on the condensation saturation curve provided by REFPROP [9]. The pressure drop across the test condenser was measured with a differential pressure transducer calibrated to an accuracy of ± 0.05 kPa. In order to calculate for energy balance, water inlet and outlet temperatures in the pre and post condensers were measured.

Table 1: Geometry of Tubes

Parameter	Microfin tube	Smooth tube
Outer diameter [mm]	9.55	9.52
Inner diameter [mm]	8.89	8.38
Mean diameter [mm]	8.67	-
Number of fins	60	-
Helix angle [$^\circ$]	37	-
Wall thickness [mm]	0.33	0.57
Fin pitch [mm]	0.45	-
Fin height [mm]	0.23	-

Data Acquisition and Experimental Procedure

All measurements of temperatures, pressure and mass flux were taken at steady state conditions when the energy balance (EB) was less than 5% and constant for a period of 5 minutes. The readings from the coriolis mass flow meters, pressure transducers and thermocouples were collected by a computerized data acquisition arrangement (DAQ) which comprised a desktop computer with LabVIEW 8.5 software. Also embedded in the DAQ were terminal blocks, channel multiplexers, termination units, transducer multiplexers, an interface card, and signal-conditioning extensions for instrumentation (SCXI). The readings were captured for 360 seconds (201 points) and the average of these was used to calculate the fluid properties, heat transfer coefficient and other important parameters. The use of the average of the 201 points was to minimize experimental errors due to noise measurement. The standard deviations of the 201 points were monitored to check for stability.

Experimental Methods and Test Conditions

A summary of the experimental parameters and uncertainties are given in Table 2. The tests were carried out at a saturation temperature of 40°C , mass fluxes (300-400kgms⁻²) and mean vapour quality (0.1-0.9). The water side rate of heat transfer rate was kept between 300 and 400 W and the uncertainties in the water side heat transfer coefficient resulted from the calibration errors on the thermocouples measuring the water temperature. The refrigerant side had dual fluctuations, one being the uncertainties in the saturation temperature and the other being uncertainties in the wall temperature. The uncertainties in the mean vapour quality was directly proportional to the energy balance and is approximately 0.05 while the uncertainties in mass flow was incorporal.

Table 2: Experimental Variables and Uncertainties

Parameter	Range	Uncertainties
T_{sat}	30-40 $^\circ\text{C}$	$\pm 0.5^\circ\text{C}$
G	300-400 kg/m ² s	± 5 kg/m ² s
x_m	0.1-0.9	± 0.05
$Q_{\text{H}_2\text{O}}$	300-400 W	10 W

DATA DEDUCTION

Eq. (1), Eq. (2) and Eq. (3) were used to calculate the energy balance, mean vapour quality and water cooling rate.

$$EB = \frac{|Q_{ref} - Q_{H_2O}|}{Q_{ref}} \quad (1)$$

$$x_m = \frac{x_{out} + x_{in}}{2} \quad (2)$$

$$Q_{H_2O} = \dot{m}_w C_p (T_{w,out} - T_{w,in}) \quad (3)$$

To determine the refrigerant properties at the entrance of the pre condenser and exit of the post condenser, temperature and pressure measurements were utilized together with the thermodynamic and thermo physical properties of the condensing fluid (R134a) which were determined by the use of a refrigerant property data base REFPROP [12]. The refrigerant vapour quality at the inlet of the test condenser x_{in} was determined from the enthalpy of the refrigerant at the inlet to the precondenser and the enthalpies of the vapour and liquid states of the refrigerants (h_l and h_v) at the same temperature and pressure conditions and is given as:

$$x_{in} = \frac{h_{test,in} - h_l}{h_v - h_l} \quad (4)$$

The enthalpy of the refrigerant at the entrance of the test section $h_{test,in}$ was determined from the enthalpy of the refrigerant at the inlet to the pre-condenser (acquired using the temperature and pressure conditions at the inlet to the pre-condenser), the rate of heat transfer, Q_{pre} and the mass flow rate of the refrigerant, \dot{m}_{ref} and is given as:

$$h_{test,in} = h_{pre,in} - \frac{|Q_{pre}|}{\dot{m}_{ref}} \quad (5)$$

The rate of heat transfer through the pre-condenser was obtained from the Eq. (6):

$$Q_{pre} = \dot{m}_w C_p (T_{pre,out} - T_{pre,in}) \quad (6)$$

The vapour quality of the refrigerant at the exit of the test section was gotten from an equation similar to Eq. (4) and is given as:

$$x_{out} = \frac{h_{test,out} - h_l}{h_v - h_l} \quad (7)$$

The enthalpy at the outlet of the test section was calculated as follows:

$$h_{test,out} = h_{test,in} - \frac{|Q_{test}|}{\dot{m}_{ref}} \quad (8)$$

Neglecting energy losses, the rate of heat transfer through the test section is same as Eq. (3) because it was assumed that the heat loss by the refrigerant during condensation equals the heat gained by the cooling water because the test section was well insulated. The coefficient of heat transfer through the test condenser which perhaps is the most important parameter was calculated from Newton's law of cooling as shown in Eq. (9)

$$\alpha_{conv} = \left| \frac{Q_{test}}{A(\bar{T}_{w,i} - T_{sat})} \right| \quad (9)$$

where A is the inner surface area of the inner tube of the test section, T_{sat} is the mean saturation temperature at the inlet and outlet of the test section, $\bar{T}_{w,i}$ is the mean inner wall temperature and it is related to the mean outer-wall temperature $\bar{T}_{w,o}$ of the tube through the thermal resistance of the wall of the copper tube R_w [K/W] as shown in Eq. (10) where R_w gotten from Fourier's law of heat conduction and is shown in Eq. (11)

$$\bar{T}_{w,i} = \bar{T}_{w,o} + |Q_{test} R_w| \quad (10)$$

$$R_w = \frac{\ln(d_o/d_i)}{2\pi k_{cu} L} \quad (11)$$

In Eq. (11), d_o and d_i are the outer and inner diameters of the inner tube of the test section and k_{cu} is the thermal conductivity of the tube wall made of copper. The average outer-wall

temperature was calculated using the trapezoidal numerical integration and is given as:

$$\bar{T}_{w,o} = \frac{1}{L} \sum_{j=1}^7 [(T_{w,o}^j + T_{w,o}^{j+1})(z_{j+1} - z_j)] \quad (12)$$

Heat transfer enhancement factor (HEF) is the ratio of the heat transfer coefficient of a microfin tube to that of a smooth tube of the same outer diameter while penalty drop factor (PF) is defined as the ratio of the pressure gradient of the microfin tube to the pressure gradient of a smooth tube. They are given in Eq. (13) and Eq. (14)

$$HEF = \frac{h_{mf}}{h_s} \quad (13)$$

$$PF = \frac{\Delta P_{mf}}{\Delta P_s} \quad (14)$$

RESULTS AND DISCUSSION

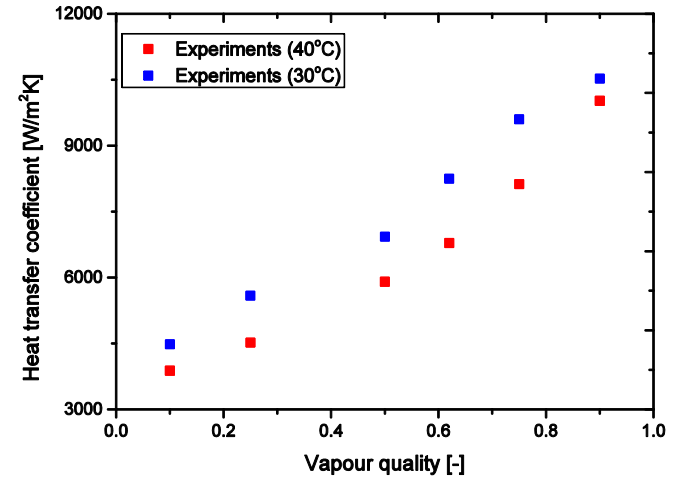


Figure 3: Influence of temperature on heat transfer coefficient of micro fin tube for horizontal flow for mass flux of 300 kg/m²s

From Fig. 3, the heat transfer coefficients were higher at a saturation temperature of 30°C [1, 7] and also increased as the vapour mean quality increased. The increase in heat transfer coefficient as saturation temperature decreased can be attributed to greater thermodynamic properties that are deemed to have an effect on heat transfer. From [12], the enthalpy of vaporization, liquid thermal conductivity, liquid thermal diffusivity, and liquid Prandtl number are greater at 30°C than 40°C. The afore-mentioned properties are related to the heat transfer coefficients.

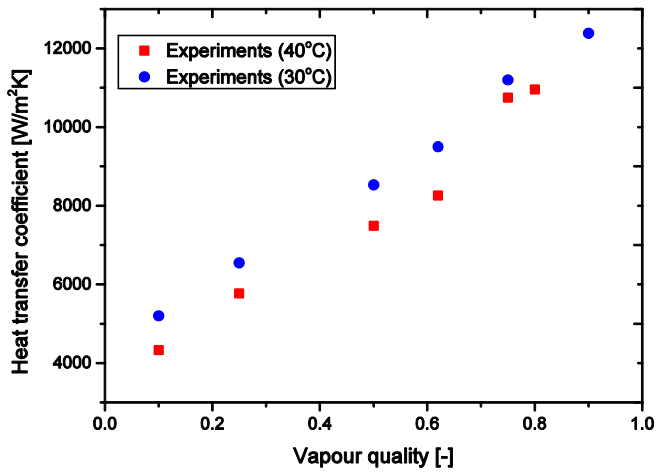


Figure 4: Influence of temperature on heat transfer coefficient for horizontal flow for mass flux of $300 \text{ kg/m}^2\text{s}$

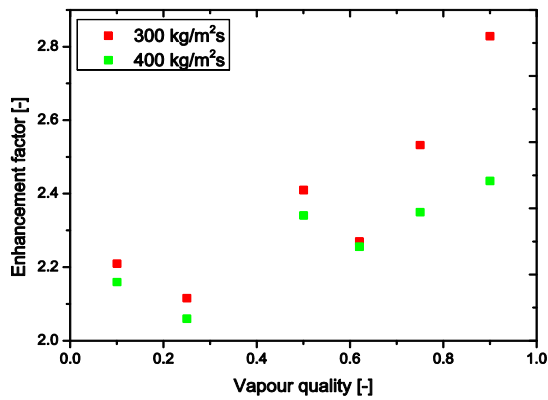


Figure 5: Enhancement factor against vapour quality for horizontal flow at 40°C

In Fig. 5, the enhancement factors ranged from 2.1 to 2.86 and were generally higher for the lower refrigerant mass flux. This can be attributed to the increase in turbulence as mass flux increased thus overwhelming the heat enhancement effect of the microfin tube relative to the smooth tube [13]. For this study, the maximum heat enhancement occurred at the high vapour quality region for both mass fluxes.

In Fig. 6, pressure drops increased with increase in mean vapour quality. In comparison with [14], our experimental results were generally higher with a deviation of 12% at a mean quality of 0.5 and 10% at mean quality of 0.8. This was expected because the helix angle of this study was greater than theirs which was 18° and the increased turbulence of flow accompanying greater helix angles.

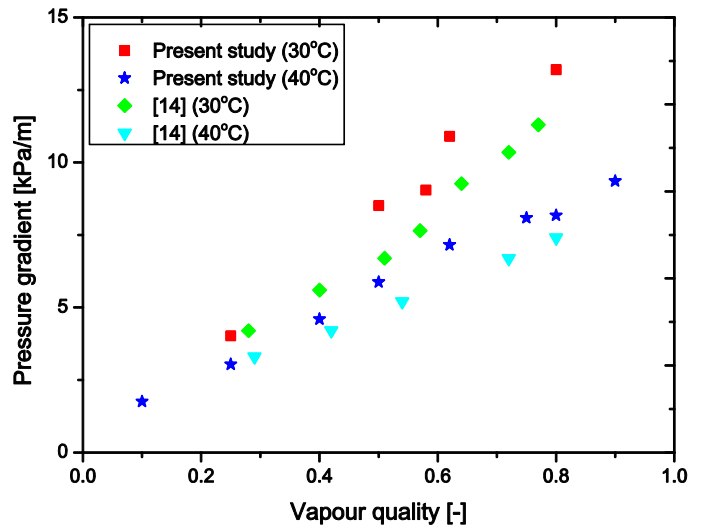


Figure 6: Influence of saturation temperature on experimental pressure drop of micro fin tube for horizontal flow for mass flux of $400 \text{ kg/m}^2\text{s}$.

The influence of saturation temperature on pressure drop was also established with pressure drop increasing as temperature decreased. The reason for this can as well be attributed to the thermodynamic properties of the working fluid at the different saturation temperatures. For instance, the surface tension which has a direct effect on pressure drop increased by 21% from 0.00613 to 0.00742 N/m as saturation temperature was altered from 40°C to 30°C . The liquid dynamic viscosity as well as density also increased with decrease in temperature and this could be responsible for the increase in pressure drop as those properties are directly proportional to pressure drops.

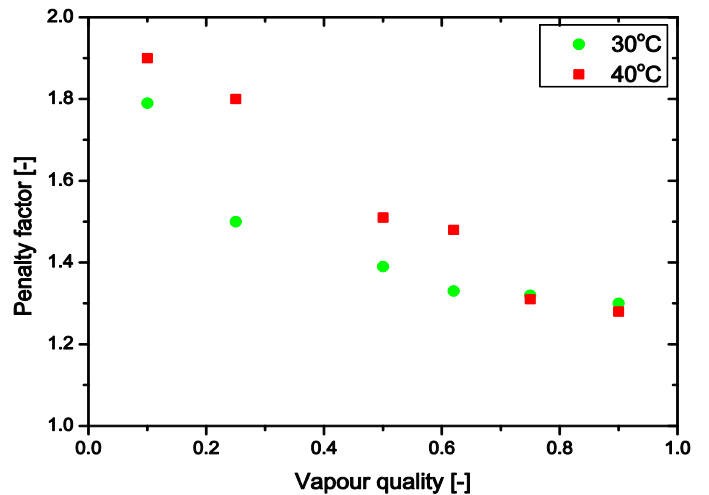


Figure 7: Penalty factor against vapour quality for horizontal flow at mass flux of $400 \text{ kg/m}^2\text{s}$

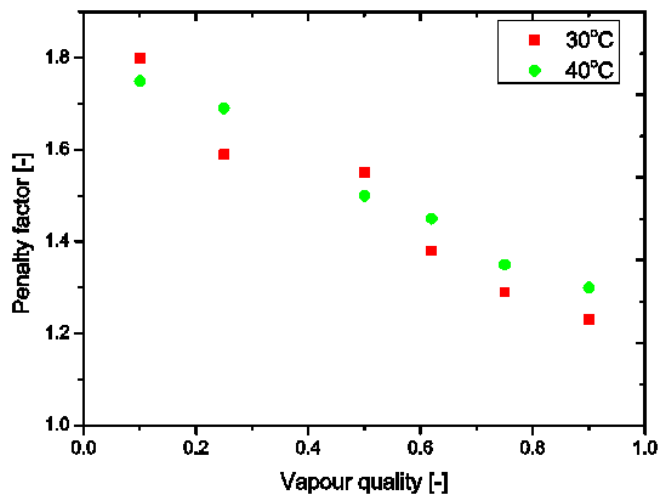


Figure 8: Penalty factor against vapour quality for horizontal flow at mass flux of $300 \text{ kg/m}^2\text{s}$

In Figures 7 and 8, the penalty drop factor varied from 1.25 to 1.8 and was higher at a saturation temperature of 30°C . This was consistent with the findings of [14] and could be attributed to increase in surface tension forces at reduced temperatures. The penalty drop factors also decreased with increase in average vapour quality and were greater at the lower mass flux. [7]. The Penalty drop factor was generally higher for a saturation temperature of 40°C and decreased as the vapour quality increased.

CONCLUSION

The results of this study are comparable to those of earlier investigations. They show substantial heat transfer enhancement and decent penalty drop factors. Heat transfer coefficients and pressure drops were greater at 30°C than 40°C . The effect of tube orientation was not considered in this study because of the mass fluxes involved wherein previous findings had showed that inclination effects were more prominent at lower mass fluxes.

ACKNOWLEDGMENT

The funding obtained from the NRF, TESP, University of Stellenbosch/ University of Pretoria, SANERI/SANEDI, CSIR, EEDSM Hub and NAC is acknowledged and duly appreciated.

REFERENCES

[1] Meyer JP, Dirker J, Adelaja AO. Condensation heat transfer in smooth inclined tubes for R134a at different saturation temperatures. *International Journal of Heat and Mass Transfer*, 2014; 70:515-525.
 [2] Lips S, Meyer P. Effect of gravity forces on heat transfer and pressure drop during condensation of R134a. *Microgravity Science Technology*, 2012; 24:157-164.

[3] Adelaja AO, Dirker J, Meyer JP. Experimental studies of condensation heat transfer in inclined microfin tube. *Proceedings of the 15th International Heat Transfer Conference, 2014*. IHTC15-9361, Kyoto Japan
 [4] Suliman R, Liebenberg L, Meyer JP. Improved flow pattern map for accurate prediction of the heat transfer coefficients during condensation of R-134a in smooth horizontal tubes and within the low-mass flux range. *International Journal of Heat and Mass Transfer*, 2009; 52: 5701–5711.
 [5] Van Rooyen E, Christians M, Liebenberg L, Meyer JP. Probabilistic flow pattern based heat transfer correlation for condensing intermittent flow of refrigerants in smooth horizontal tubes. *International Journal of Heat and Mass Transfer*, 2010; 53: 1446-1460.
 [6] Akhavan-Behadabi MA, Kumar R, Mohseni SG. Condensation heat transfer of R-134a inside a micro-fin tube with different tube inclinations. *International Journal of Heat and Mass Transfer*, 2007; 50: 4864-4871.
 [7] Eckels SJ, Tesene BA. A comparison of R-22, R-134a, R-410A and R-407C condensation performance in smooth and enhanced Tubes: Part 1, Heat Transfer. *ASHRAE Transactions*, 1999; 105: 428–441.
 [8] Kim MH, Shin JS. Condensation heat transfer of R22 and R410A in horizontal smooth and microfin tubes. *International Journal of Refrigeration*, 2005; 28: 949–957.
 [9] Jung D, Cho Y, Park K. Flow condensation heat transfer coefficients of R22, R134a, R407C and R410A inside plain and microfin tubes. *International Journal of Refrigeration*, 2004; 27:25-32.
 [10] Mussio A, Niro A, Arosio S. Heat transfer and pressure drop during condensation of R22 inside 9.52mm OD. microfin tubes of different geometries. *Enhanced Heat Transfer*, 1998; 5: 39-52.
 [11] Nualnoonrueng T, Kaewon J, Wongwises S. Two phase condensation heat transfer coefficients of hfc-134a at high mass flux in smooth and microfin tubes. *International Communications in Heat and Mass Transfer*, 2003; 28, 4:577-590.
 [12] REFPROP. NIST Thermodynamic properties of refrigerants and refrigerant mixtures, version 8.0, NIST Standard Reference Database 23, 2005.
 [13] Bukasa JP, Liebenberg, L, Meyer, JP. Influence of spiral angle on heat transfer during condensation inside spiralled micro-fin tubes. *Heat Transfer Engineering*, 2005; 26, 7: 11-21.
 [14] Nualnoonrueng T, Kaewon J, Wongwises S. Two phase flow pressure drop of hfc-134a during condensation in smooth and micro fin tubes at high mass flux. *International Communications in Heat and Mass Transfer*, 2004; 31, 7:991-1004.